Received: 25 August 2020 | Revised: 29 October 2020 | Accepted: 15 January 2021

DOI: 10.1002/alz.12305

Alzheimer's & Dementia®
THE JOURNAL OF THE ALZHEIMER'S ASSOCIATION

FEATURED ARTICLE

Plasma hydrogen sulfide: A biomarker of Alzheimer's disease and related dementias

Elizabeth Disbrow[1,2,3,4] | **Karen Y. Stokes**[2,3,5] | **Christina Ledbetter**[2,6] | **James Patterson**[2,7] | **Roger Kelley**[1,2] | **Sibile Pardue**[3] | **Tyler Reekes**[2,4] | **Lana Larmeu**[2,6] | **Vinita Batra**[2,7] | **Shuai Yuan**[8] | **Urska Cvek**[9] | **Marjan Trutschl**[9] | **Phillip Kilgore**[9] | **J. Steven Alexander**[1,2,3,5] | **Christopher G. Kevil**[2,3,10]

[1] Department of Neurology, LSU Health Shreveport, Shreveport, Louisiana, USA

[2] Center for Brain Health, LSU Health Shreveport, Shreveport, Louisiana, USA

[3] Center for Cardiovascular Diseases and Sciences, LSU Health Shreveport, Shreveport, Louisiana, USA

[4] Department of Pharmacology, LSU Health Shreveport, Shreveport, Louisiana, USA

[5] Department of Molecular and Cellular Physiology, LSU Health Shreveport, Shreveport, Louisiana, USA

[6] Department of Neurosurgery, LSU Health Shreveport, Shreveport, Louisiana, USA

[7] Department of Psychiatry and Behavioral Medicine, LSU Health Shreveport, Shreveport, Louisiana, USA

[8] Vascular Medicine Institute, University of Pittsburgh Medical Center, Pittsburgh, Pennsylvania, USA

[9] Dept. of Computer Science, Laboratory for Advanced Biomedical Informatics, Louisiana State University Shreveport, Shreveport, Louisiana, USA

[10] Department of Pathology and Translational Pathobiology, Department of Pathology, and Cell Biology and Anatomy, LSU Health Shreveport, Shreveport, Louisiana, USA

Correspondence
Elizabeth Disbrow, PhD, Associate Professor, Department of Neurology, LSU Health Shreveport LA 71130-3932, USA.
Email: edisbr@lsuhsc.edu

Funding information
National Institutes of General Medical Sciences National Institutes of Health, Grant/Award Numbers: 3P2012130701A1S1, HL149264

Abstract

While heart disease remains a common cause of mortality, *cerebrovascular* disease also increases with age, and has been implicated in Alzheimer's disease and related dementias (ADRD). We have described hydrogen sulfide (H_2S), a signaling molecule important in vascular homeostasis, as a biomarker of cardiovascular disease. We hypothesize that plasma H_2S and its metabolites also relate to vascular and cognitive dysfunction in ADRD. We used analytical biochemical methods to measure plasma H_2S metabolites and MRI to evaluate indicators of microvascular disease in ADRD. Levels of total H_2S and specific metabolites were increased in ADRD versus controls. Cognition and microvascular disease indices were correlated with H_2S levels. Total plasma sulfide was the strongest indicator of ADRD, and partially drove the relationship between cognitive dysfunction and white matter lesion volume, an indicator of microvascular disease. Our findings show that H_2S is dysregulated in dementia, providing a potential biomarker for diagnosis and intervention.

KEYWORDS
ADAS-cog, brain volume, Cognitive function, FLAIR, H2S, MRI

1 | PART I. NARRATIVE

Because Alzheimer's disease (AD) is the most common form of age-related neurological disability, identifying, and treating its underlying causes is a critical health challenge. The etiology of AD is complex and multifactorial, and there is accumulating evidence that cerebrovascular dysfunction makes a significant contribution to dementia pathophysiology. While the amyloid cascade hypothesis suggests that accumulation of amyloid "plaques" and phosphorylated-Tau (p-Tau) "tangles" play mechanistic roles in AD,[1,2] therapies targeting suppression of these factors have not yet proven widely clinically effective.[2] However, there is evidence linking the accumulation of amyloid and p-Tau with cerebrovascular dysfunction.[3] Cerebrovascular disease has been reported in up to 70% of dementia patients upon postmortem examination,[4,5] underlining the link between the two. Furthermore, the incidence of both dementia and stroke appear to be increasing in tandem worldwide,[6] reflecting socioeconomic status and its influence on largely modifiable *vascular* risk factors. The "*vascular dysregulation hypothesis*"[7–9] proposes that imbalances between blood flow-based substrate delivery and brain energy requirements intensify common cardiovascular risks for Alzheimer's disease and related dementias (ADRD) including hypertension,[10–12] cerebrovascular disease[13–15], and sedentary lifestyle.[16,17] The current thinking is that cerebrovascular dysfunction occurs early in ADRD,[6] and therefore may be an earlier diagnostic marker and a more fruitful therapeutic target.

I Similarly, a recent review by Emrani et al. concluded that vascular risk factors represent initial *precedent* insults.[18] For instance, in ADRD, vascular dysfunction can drive inflammation which weakens the blood brain barrier (BBB), potentially initiating a cascade of pathophysiologies leading to AD progression. Specifically, disturbances in BBB integrity may set off a cascade of events including excitotoxic calcium signaling (the "*calcium hypothesis" of AD*[19–21]) and metabolic stresses which progressively damage brain structure/function and culminate in amyloid plaques and p-Tau tangles (see Hachinski[6] for review). Consequently, AD and vascular dementia appear to be overlapping and potentially linked clinical phenomena, rather than discrete disease categories.[18] In fact, Hachinski et al. ([6], see Figure 3) proposed modifying the *"Jack"* model of Alzheimer's disease[22] to embrace the cerebral vasculature as an early ADRD target in addition to beta amyloid and Tau. Further, the importance of vascular contributions to ADRD was recently recognized by the National Institute on Aging and the Alzheimer's Association. While brain imaging and cerebrospinal fluid analyses were included in the NIAA comprehensive AT(N) (amyloid, p-Tau, and neurodegeneration) biomarker panel, in 2018 the NIAA recommended adding *vascular biomarkers* to this panel.[23] Here, we hypothesize that plasma hydrogen sulfide (H_2S) represents a novel *vascular* biomarker whose concentration is tightly associated with cognitive dysfunction and disease activity in ADRD.

HIGHLIGHTS

- We used novel biochemical methods to measure plasma hydrogen sulfide metabolites in ADRD.
- Levels of total H_2S and specific metabolites were increased in ADRD versus controls.
- Cognition, brain volume, and microvascular disease indices were correlated with H_2S levels
- H_2S is dysregulated in dementia, providing a potential biomarker for diagnosis and intervention.

RESEARCH IN CONTEXT

1. Systematic review: The authors reviewed the literature using traditional sources including PubMed, Web of Science and Google Scholar, as well as meeting abstracts from the Society for Neuroscience and the International Society for Neurovascular Disease. Previous work on hydrogen sulfide and its metabolites has focused on the cardiovascular system. ADRD are intensively studied research targets. We have set our work in the context of this existing research and the relevant citations are appropriately cited.
2. Interpretation: Our findings suggest that plasma hydrogen sulfide is elevated in dementia and is strongly correlated with cognitive dysfunction. Furthermore, hydrogen sulfide mediated the relationship between cognitive dysfunction and MRI measures of chronic cerebral microvascular disease.
3. Future directions: Our study indicates that hydrogen sulfide is an important biomarker of cognitive dysfunction in ADRD. This finding suggests new hypotheses and warrants the pursuit of additional studies such as: (a) determining the specificity of these markers for ADRD over other neurodegenerative diseases, (b) examining longitudinal relationships between hydrogen sulfide and cognitive decline in AD, and (c) evaluating therapeutic benefits of altering hydrogen sulfide metabolism on the course of ADRD disease activity.

1.1 | Hydrogen sulfide and its metabolites in vascular dysfunction and neuropathology

There is a growing appreciation for the roles of H_2S and its metabolites in the regulation of both vascular and neuronal homeostasis.[24,25]

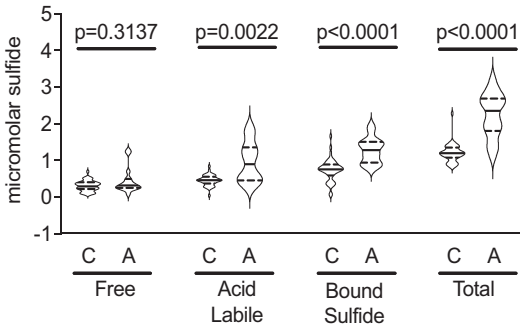

FIGURE 1 Violin plot of the median and distribution densities of plasma H_2S metabolite measures in control (C) and Alzheimer's Disease related dementia (A) participants. The violin plot is a nonparametric representation of all data points. The solid line is the group median, while the width of each plot represents subject density. Dashed lines indicate the interquartile range

Plasma H_2S and its metabolites have been well described as vascular disease blood biomarkers,[26] and recent work indicates that imbalances in H_2S metabolism exist in the vascular compartment during several disease states.[24] In the brain, H_2S acts as a neurotransmitter/second messenger produced following nerve excitation,[27] and modulates NMDA receptors during long term potentiation[28] for memory consolidation. Several cell types within the brain and its vasculature generate H_2S from cysteine.[29] In the brain parenchyma, H_2S is produced by the enzyme cystathionine β-synthase (CBS), while cystathionine γ-lyase (CSE) generates H_2S derived from cerebral microvessels. Additionally, three biochemical forms of reactive sulfur pools exist: free H_2S, acid-labile (eg, iron-sulfur clusters) and bound sulfide (eg, persulfides, polysulfides).

We and others have previously described defensive roles for H_2S in preserving normal brain vasomotion,[30,31] and cognitive function in experimental models of dementia.[32 33–35] Conversely, H_2S and its metabolites have been shown to contribute to neurological stress and vascular dysfunction, a deleterious role consistent with our current findings. Here, for the first time we have shown that plasma H_2S and H_2S metabolites are elevated in ADRD (Figure 1), and levels were associated with both cognitive dysfunction and neuroimaging evidence of microvascular disease (Figure 2). Neuroimaging evidence of microvascular disease is indirect and includes FLAIR white matter lesion volume and brain volume measures of atrophy.[36] These findings indicate that the link between H_2S imbalance and ADRD may be due, at least in part, to microvascular dysfunction. When we tested this possibility using mediation analysis (Figure 2**D**), results indicated that H_2S drove half of the relationship between cognitive dysfunction and white matter lesions, an indicator of microvascular disease. In addition, H_2S and its metabolites had significant ADRD diagnostic utility (Figure 3), and classifier analysis revealed that total plasma sulfide burden was the best indicator of ADRD. A threshold of 1.64 μM plasma H_2S yielded a classification accuracy = 0.930 and a sensitivity of 0.80 (Figure 4). It is noteworthy that plasma H_2S alone was a powerful discriminator between ADRD and controls, and that a combined approach, including imaging and demographic data, did not further improve the sensitivity and specificity of our decision tree classification model.

The apparent contradictory findings for the role for H_2S in brain-related pathologies are consistent with literature on other gasotransmitters such as nitric oxide, where in some pathologies excess nitric oxide has been shown to be deleterious, while in others decreased nitric oxide bioavailability has been reported.[37,38] The fact that both too little and too much H_2S can be detrimental to brain health may represent a neuroprotective system that breaks down under pathological conditions. Our work is consistent with studies of Downs' syndrome, a condition with several AD-related features and mechanisms, where *elevated* H_2S production has been observed.[39] Schizophrenia models also show elevated levels of the H_2S/polysulfide producing enzyme "Mpst", and C3H schizophrenic mice which display behavioral deficits show elevated sulfides,[40] suggesting that "*sulfide stress*" contributes to cognitive dysfunction.

These previous studies support our hypothesis that H_2S may become dysregulated in ADRD, where vascular and cognitive functions are intimately linked. One possible mechanism through which H_2S levels are elevated is suggested by the "vascular dysregulation hypothesis," which predicts that cerebral hypoxia contributes to ADRD pathogenesis. Because hypoxia and ischemia are potent inducers of CSE expression and function,[41,42] age-related vascular deficits in brain oxygenation implicate CSE activity in neuronal dysfunction, particularly in areas of the brain where oxygenation is compromised.[43] Furthermore, hypertension and disturbances in cerebrovascular flow, often seen in ADRD[44] may enhance CSE expression and activity[45,46] and increase "bound" polysulfide pools. Thus, oxygenation abnormalities may drive H_2S links to a "vascular dysregulation hypothesis," and anticipate associations between the vascular dysfunction observed in the brain and alterations in circulating H_2S metabolites in ADRD.

1.2 | Pathways through which hydrogen sulfide disrupts brain microvasculature

How might ADRD disease activity, cognitive dysfunction and neuroimaging be related to sulfides? The answer may lie in early, "silent" BBB disturbances driven by abnormal H_2S homeostasis. Our group, over the last decade, has investigated several gasotransmitters including H_2S, nitric oxide and their metabolites as contributors to *vascular endothelial barrier* failure.[47] We showed that exogenous polysulfide donors (not free sulfide donors) act on endothelial junctions to *depress* vascular barrier in vitro. We have evidence that such a damaging role for H_2S metabolites also applies to the BBB, where barrier disruption early after stroke is mediated by H_2S species.[30] Specifically, our reports on the impact of H_2S on the brain vasculature revealed a role for CSE-derived H_2S metabolites in ischemic stroke induced vasodilation/hyperemic response and barrier permeability early during reperfusion.[30] It should be noted that polysulfides can be generated endogenously both by the oxidation of H_2S, and directly from CSE. Therefore, we examined the role of CSE in basal vascular integrity. Using CSE-deficient mice, we observed a significant reduction in small

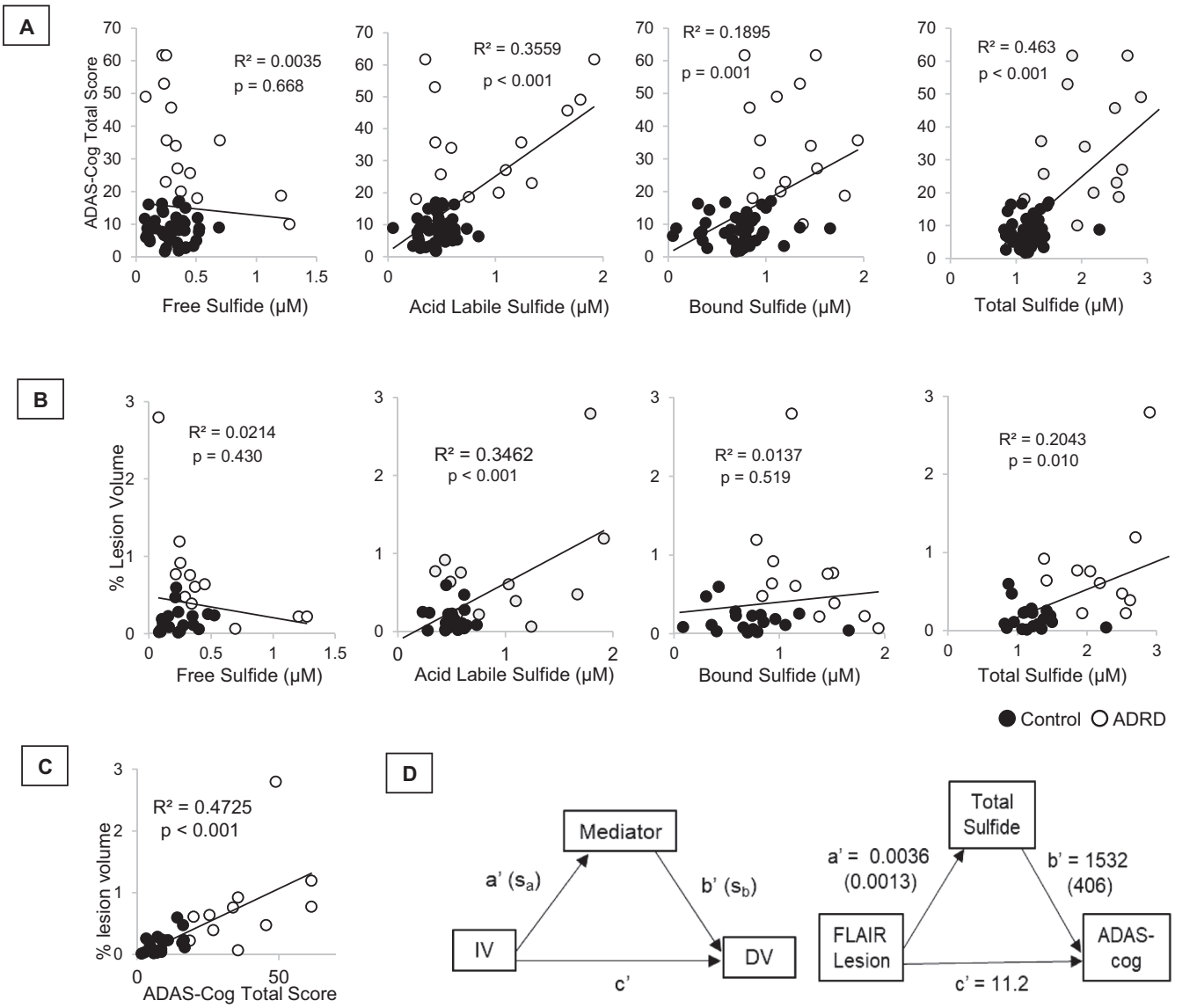

FIGURE 2 Scatterplots of cognitive function, H_2S and lesion volume outcomes. Strong relationships were observed between H_2S metabolites (particularly acid labile and total sulfide) and both the cognitive outcome measure (A) and an indicator of chronic microvascular disease (B). (C) Scatterplot showing the strong relationship between cognitive function and an indicator of microvascular disease. (D) Model of mediation analysis (left) and mediation analysis results (right). Total sulfide mediated the relationship between the measure of cognitive function and an indicator of chronic microvascular disease

solute (sodium fluorescein) permeability in the brain, indicating that the barrier function was enhanced in the absence of CSE. This effect was not specific to the brain, as we saw a similar response in the lungs (Figure 5). This multi-organ finding, along with the fact that CSE is primarily found in the vasculature, represents a first step in proving our hypothesis that a vascular source of CSE-derived H_2S is responsible for the imbalance in H_2S homeostasis in ADRD.

Although still in need of larger studies, our findings are consistent with a scheme where elevated levels of H_2S and its metabolites drive barrier disturbances which underlie excitotoxic stress and cognitive injury, particularly in ADRD.[48] In ADRD, disturbances in brain endothelial barrier function can flood the brain interstitium with toxic neurotransmitters, immune components, and iron, each potentially able to trigger a progressive, and calcium-dependent, excitotoxicity ("calcium hypothesis"[6,19–21]). Over the course of years, these changes could lead to structural and functional derangement seen in longstanding ADRD. Our findings reveal that sulfide stress may represent an important indicator of ADRD disease activity which links brain vascular disturbances to cognitive dysfunction, and could provide valuable novel diagnostic, prognostic, and mechanistic insights into ADRD.

1.3 | Limitations

We recognize that this study is limited by participant AD diagnosis that is unconfirmed by autopsy. However, even with the possible

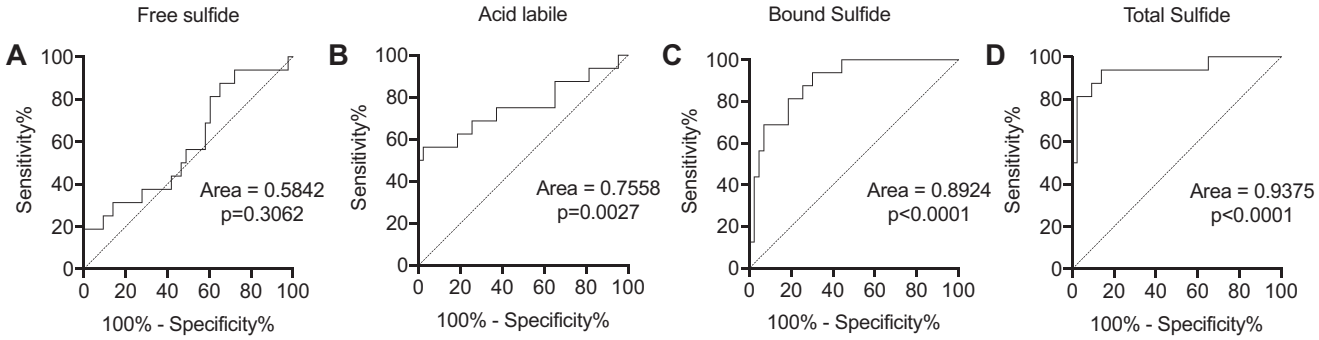

FIGURE 3 Receiver-operating characteristic (ROC) curve analysis demonstrate that H_2S metabolites are indicators of ADRD. Panel A reports ROC of free sulfide, panel B shows ROC for acid labile sulfide, panel C illustrates ROC for bound sulfide, and panel D shows ROC for total sulfide. Area = area under the curve

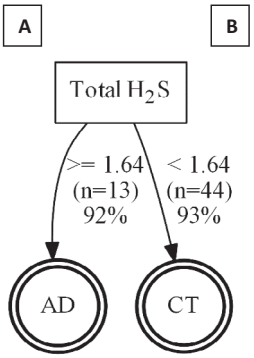

Variable	All	Total H_2S Metabolites	All (N=MRI-only)	Total H_2S (N=MRI-only)
Accuracy	0.929825	0.929825	0.903226	0.903226
Sensitivity	0.8	0.8	0.833333	0.833333
False Neg. Rate	0.2	0.2	0.166667	0.166667
Specificity	0.97619	0.97619	0.947368	0.947368
False Pos. Rate	0.02381	0.02381	0.052632	0.052632
Pos. Pred. Value	0.923077	0.923077	0.909091	0.909091
False Disc. Rate	0.076923	0.076923	0.090909	0.090909
False Omit. Rate	0.068182	0.068182	0.1	0.1
Neg. Pred. Value	0.931818	0.931818	0.9	0.9
Candidate Dimensions	10	5	10	5

FIGURE 4 Tree Classifier. (A) Decision tree showing total sulfide as the most effective classifier, with a cut off value of 1.64 μM H_2S; AD: Alzheimer's Disease related dementia; CT: control. (B) Classifier performance metrics for the tree classifier according to their ability to predict diagnosis (see methods for description of classifier metrics). A single dimension was chosen (Total Sulfide) by the classifier despite the number of candidate dimensions. We also ran the analysis using only the records containing MRI data for comparison (MRI-only). The "All" and "Total H_2S" facets have duplicated accuracy statistics because in both of these, the same decision tree was generated. We used several measures to classify the accuracy of the classifier. Accuracy describes the probability that the classifier arrives at a correct prediction. Sensitivity describes the probability of correctly predicting a positive condition. Specificity describes the probability of correctly predicting a negative condition. False negative rate and false positive rate indicate the failure of the classifier to correctly categorize positive or negative conditions. Positive predictive value and Negative predictive value represent the reliability of a positive or negative condition respectively. False discovery rate and False omission rate represent the probability that the respective predicted condition does not represent the actual condition

heterogeneity of our dementia group, the H_2S discriminatory power was exceptionally high. Though the groups were small, they were a highly studied cohort of individuals showing a remarkable and mathematically compelling relationship between total H_2S (primarily bound and acid labile pools) and cognitive dysfunction, indicating that larger studies would likely recapitulate these findings. Nevertheless, the small sample leaves the findings vulnerable to confounding factors that are associated with H_2S, ADRD pathology, cerebrovascular disease, or cognitive dysfunction. It remains to be seen if total H_2S and/or specific H_2S metabolites are general markers of neurodegeneration or if they are ADRD-specific. Other questions that remain unanswered due to the limited number of participants include examination of relevant disease subgroups such as comorbidity, sex, or race-based cohorts. Nonetheless, our findings that H_2S metabolites provide higher diagnostic performance than even blood β-amyloid secondary structures, despite the very limited number of individuals, strongly supports pursuit of this approach in larger studies that can evaluate limitations, delineate prospective changes in disease and sulfides, and provide improved patient stratification.

1.4 | Future directions for hydrogen sulfide as a biomarker for ADRD

Our initial biomarker studies are highly promising. The well-defined association between blood H_2S levels and microvascular disease suggest the testable hypothesis that increased generation of H_2S from CSE, abundant in cerebral microvessels, may drive ADRD progression. Our results showed that total sulfide mediated the relationship between cognitive performance and microvascular related outcomes,

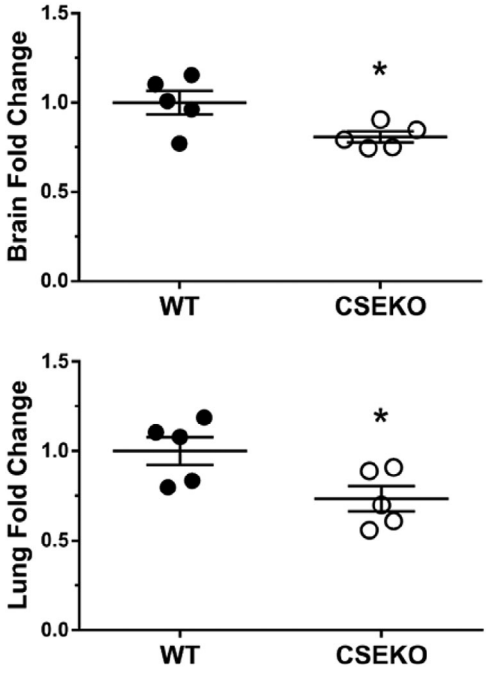

FIGURE 5 CSE knockout mice exhibit reduced vascular permeability. Sodium fluorescein permeability was significantly reduced in the brains (top) and lungs (bottom) of CSE knockout mice compared to wild type controls (*significant $P < .05$, student's t-test, n = 5/group)

supporting a causal role for H_2S dysregulation in ADRD. Our study indicates that at least some of these H_2S metabolites, such as oxidized H_2S, may accumulate in the circulation with deleterious consequences. The fact that powerful group discrimination could be obtained using only a single plasma analyte is remarkable in the ADRD field. These findings suggest further steps are warranted to verify biomarker sensitivity and specificity (see Frisoni et al. Table 3[49]).

The specificity of H_2S as a marker of AD as opposed to other forms of dementia, as well as other proteinopathies such as Parkinson disease remains to be determined. Our work also anticipates longitudinal studies for the evaluation of early detection and progression monitoring. The linear nature of the relationships among cognitive, brain volume, and lesion volume measures with total sulfide, as well as acid-labile and bound sulfide pools suggest that H_2S metabolites may reflect disease progression and could thus have prognostic value. Determining the required interval to detect change for repeated testing, and marker efficacy for early detection are critical goals of future studies for biomarker identification. Based on our observations, it is possible that modulation of plasma sulfides might also represent a therapeutic opportunity in ADRD. It is not clear whether our results will reveal "at-risk" individuals who may go on to develop earlier or more severe disease. However, if modifiable risk factors do contribute to ADRD progression, earlier intervention in such "at-risk" individuals could limit or prevent inevitable progression into clinical ADRD. Because blood sampling remains the easiest, most repeatable and inexpensive method of evaluating biospecimens, reliable blood-based diagnostics for ADRD, as described here, would have an enormous impact in combatting ADRD.

2 | PART II. CONSOLIDATED RESULTS AND STUDY DESIGN

2.1 | Hydrogen sulfide and its metabolites in ADRD and associated cognitive impairment

The physiology of H_2S and H_2S metabolites in ADRD and related neuropathology is not well understood. Since the most accessible pools of H_2S are in the circulation, our first step was to determine if plasma levels of H_2S and its metabolites were different in people with and without ADRD. We enrolled 15 participants with ADRD and 42 controls for cognitive and blood testing, and, of these, 12 ADRD and 19 control participants also had MRI (Table 1). We found that total H_2S levels increased with ADRD, and that this increase was primarily due to elevations in both acid-labile and bound sulfide pools, not free sulfide (Figure 1). This finding is in contrast to our observations from cardiovascular disease, showing a decline in plasma total, bound, and acid-labile H_2S levels,[50] thus suggesting a disease mechanism that is unique to the brain. Furthermore, our findings disagree with the only previous study on H_2S in human AD and vascular dementia, which reported decreased H_2S levels in plasma.[51] While these apparently conflicting results are consistent with a dual role for H_2S where both deficient and excessive levels are pathological, our findings also indicate that a redistribution between H_2S pools may be a critical determinant in the pathological consequences, which none of the previous studies have measured. However, it is also possible some of these conflicting findings relate to the populations studied or the methods used to measure H_2S. We used an advanced "state of the art" precise method of H_2S measurement developed by our group which was designed to address limitations of the method used by many others.[50,52,53]

Of importance from a mechanistic perspective was whether circulating H_2S metabolite levels correlated with cortical volume and/or white matter lesion volume, both indicators of microvascular health. To better understand the relative roles for H_2S in these two interrelated components of ADRD, we used typical diagnostic indices, and correlated them with plasma H_2S levels. MRI has been widely applied to identify cerebral ventricular and hippocampal volumes as a measure of AD status [39–41]. As expected, our ADRD population showed decreased hippocampal and increased ventricular volumes. While neither of these indices correlated with levels of H_2S or individual sulfide pools, there was a clear, inverse relationship between total brain volume and H_2S levels (Table 2). In addition, the MRI based lesion outcome measure was strongly correlated with both acid-labile and total H_2S (Table 2).

Of primary importance from a clinical perspective was quantifying the cognitive impairment that characterizes ADRD. Using the Alzheimer's disease Assessment Scale (ADAS-Cog) score as a measurement of cognitive function, we linked higher ADAS-Cog scores in ADRD, indicative of cognitive dysfunction, with higher H_2S levels in

TABLE 1 Demographic data for the total sample (Total) and the MRI subgroups (MRI)

	N	Age (years)	Education (years)	ADAS Score*
ADRD Total	15 (13 female, 7 AA)	68.47 (5.93)	14.80 (2.68)	34.65 (16.31)
Control Total	42 (36 female, 19 AA)	67.50 (9.65)	15.90 (2.16)	8.40 (4.25)
ADRD MRI	12 (10 female, 7AA)	67.42 (4.10)	14.00 (2.24)	35.38 (16.50)
Control MRI	19 (16 female, 12 AA)	63.47 (7.54)	16.15 (2.21)	8.85 (5.00)

Our total sample was predominantly female (ADRD = 86.7% vs Control = 85.7%). About half of the participants were African American (AA; ADRD = 53.8% and Control = 52.7%) and the other half were white. Proportions were similar for the MRI subgroups.
*$P < .001$ for ADRD versus control groups.

the plasma. In fact, the ADAS-Cog correlated very tightly not only with total H_2S, but also with both acid-labile and bound sulfide pools. To examine the causal relationship among cognitive function, white matter lesion volume and H_2S, we further employed mediation analysis. Specifically, we examined the contribution of H_2S to the relationship between cognitive function and an indicator microvascular disease. Total H_2S was found to drive half of the effect of lesion volume on cognitive function (Figure 2**D**). This finding indicates that H_2S metabolites may be mechanistically significant as a contributor to ADRD. Importantly, these findings are consistent with cognitive and structural disturbances related to sulfides that originate in the vascular space and act to disrupt vascular homeostasis, leading to downstream neurodegeneration.

2.2 | Sensitivity and specificity of sulfides in ADRD

ADRD diagnostic tools remain somewhat unreliable and differ in their specificity and sensitivity. The current mainstay of AD diagnosis, the ADAS-cog score has good sensitivity and specificity at 90.09% and 85.88% respectively [21]. While widely applied, ADAS-cog requires trained operators, is time-consuming and is subject to variability based on patient performance. Hippocampal and ventricular changes on MRI also predict disease activity [42]. Although we found significant diagnostic performance for acid-labile, bound, and total sulfide (Figure 3), greater discriminative ability was noted with total sulfide (AUC = 0.94, 95% confidence interval: 0.92 to 1.000; **panel 3D**). Plasma β-amyloid has also been widely studied as an AD biomarker [43]; its use in receiver operator characteristic (ROC) curve analysis discriminated AD patients from controls with a specificity/sensitivity of 91% and 71% respectively (AUC = 0.80). Overall, its diagnostic accuracy was good, but not ideal (86%) [43]. The problem with such approaches is that AD diagnosis still remains probabilistic, with the most definitive confirmation only available at autopsy.[54,5] Low diagnostic accuracy in AD may be related to its complex nature, long course, and variable etiopathogenesis. Thus, the most accurate approach may be a biomarker panel.

For example, Brickman et al.[56] noted that cerebrovascular disease and brain atrophy often overlap, and reported that the addition of MRI measures of infarcts and white matter integrity improved the fit of their quantitative MRI index over cortical measures alone. Furthermore, Fink et al.[44] showed that combining amyloid PET, $^{18-}$F FDG PET, and CSF tests improved specificity/sensitivity for distinguishing neuropathologically-defined AD from non-AD in older adults with dementia. In order to maximize the discriminative power of our blood, MRI and behavioral data, we performed classification analysis to create a decision tree.[57]

A decision tree analysis yields a graphic representation of alternative solutions based on probability analysis. We included all MRI and H_2S variables as indicators of ADRD. This analysis provided a decision tree that had a single level consisting of total sulfide (Figure 4**A**). The tree had an accuracy of 93.0%, a sensitivity of 80%, a positive predictive value of 92.3% and a negative predictive value of 93.2% (Figure 4**B**). These findings indicate that total H_2S *alone* accurately reflects the contribution of brain volume, white matter lesion and H_2S metabolite abnormalities to cognitive disturbance in ADRD. While it remains to be seen if the addition of β-amyloid or p-Tau outcomes can improve diagnostic power of total plasma H_2S, our findings reveal that H_2S, when used alone, is a very powerful predictor of ADRD.

3 | PART III. DETAILED METHODS AND RESULTS

3.1 | Methodological and technical specifics of human studies

3.1.1 | Subjects

Written informed consent was obtained according to the policy of the institutional review board of Louisiana State University Health Sciences Center, Shreveport. We studied 16 individuals who met the criteria for "ADRD" (ADAS-cog score > 17 or clinical diagnosis of AD (1 subject, ADAS-cog score = 10)) and 42 age-similar controls. Inclusion criteria were age > 50 years (mean 67.8 yrs.) with English as their primary language. A subset of participants (n = 12 ADRD, 19 controls) met inclusion/exclusion criteria and underwent MRI. Cognitive evaluation (ADAS-cog) tests, and blood draws were performed at the same visit, with MRI performed an average of 42 days after neuropsychological testing.

3.1.2 | Cognitive assessments

Cognitive status was evaluated using the MMSE. Dementia was defined as an ADAS-cog score of > 17.[58] The total session duration was 2-4 hours.

TABLE 2 Correlation matrix of demographic, cognitive, MRI, and H_2S variables

Edu.	ADAS	Brain Vol.	Hippo. % Vol.	Ventricle % Vol.	Gray % Vol.	White % Vol.	Lesion % Vol.	Plasma Free H_2S	Acid Labile H_2S	Plasma Bound H_2S	Plasma Total H_2S		
0.172	0.036	−0.339	−0.053	0.252	0.078	−0.055	0.170	0.205	−0.189	0.065	−0.077	Corr.	Age
0.200	0.792	0.062	0.778	0.172	0.675	0.769	0.359	0.126	0.158	0.630	0.567	Sig.	
57	57	31	31	31	31	31	31	57	57	57	57	N	
	−0.125	.398*	0.280	−0.059	0.253	−0.224	−.394*	−0.098	−.371**	−0.110	−.314*	Corr.	Edu.
	0.353	0.027	0.127	0.752	0.169	0.226	0.028	0.467	0.004	0.415	0.018	Sig.	
	57	31	31	31	31	31	31	57	57	57	57	N	
		−.378*	−.418*	.727**	−0.343	0.334	.687**	−0.059	.596**	.436**	.681**	Corr.	ADAS
		0.036	0.019	0.000	0.059	0.067	0.000	0.664	0.000	0.001	0.000	Sig.	
		31	31	31	31	31	31	57	57	57	57	N	
			0.013	−.378*	0.051	−0.008	−0.274	0.011	−0.253	−0.299	−.361*	Corr.	Brain Vol.
			0.943	0.036	0.787	0.964	0.136	0.953	0.169	0.102	0.046	Sig.	
			31	31	31	31	31	31	31	31	31	N	
				−.368*	.406*	−.455*	−0.320	0.044	−0.186	−0.056	−0.155	Corr.	Hippo. % Vol.
				0.042	0.023	0.010	0.079	0.814	0.317	0.767	0.405	Sig.	
				31	31	31	31	31	31	31	31	N	
					0.017	−0.006	.494**	−0.114	0.212	0.200	0.269	Corr.	Ventricle % Vol.
					0.928	0.973	0.005	0.543	0.252	0.281	0.144	Sig.	
					31	31	31	31	31	31	31	N	
						−.990**	−.416*	0.253	−0.303	−0.009	−0.199	Corr.	Gray % Vol.
						0.000	0.020	0.169	0.097	0.960	0.284	Sig.	
						31	31	31	31	31	31	N	
							.399*	−0.231	0.266	0.002	0.170	Corr.	White % Vol.
							0.026	0.212	0.149	0.992	0.361	Sig.	
							31	31	31	31	31	N	
								−0.146	.588**	0.117	.452*	Corr.	Lesion % Vol
								0.433	0.000	0.530	0.011	Sig.	
								31	31	31	31	N	
									−0.129	.429**	0.210	Corr.	Plasma Free H_2S
									0.338	0.001	0.118	Sig.	
									57	57	57	N	
										0.139	.738**	Corr.	Plasma Acid Labile H_2S
										0.304	0.000	Sig.	
										57	57	N	
											.771**	Corr.	Plasma Bound H_2S
											0.000	Sig.	
											57	N	

*$P < .05$.
*$P < .01$.

3.1.3 | Hydrogen sulfide analysis

Blood was collected in lithium-heparin vacutainer tubes and processed within 15 minutes. Samples were centrifuged at 1400 RCF for 4 minutes. Plasma was combined in a 5:1 ratio of plasma to stabilization buffer (degassed 100 mM Tris–HCl buffer, pH 9.5, 0.1 mM diethylene triamine pentaacetic acid), quickly frozen, and stored in liquid nitrogen until analysis. The sulfide pools were isolated according to analytical high pressure liquid chromatograph (HPLC) procedures previously established in our lab.[53] Derivatization of sulfide with excess monobromobiamine was performed under specific reaction conditions for all three pools (free, acid-labile, and bound) using the monobromobiamine method of Shen et al.[52] Each evaluation was performed in triplicate.

3.1.4 | Brain imaging

Participants underwent a 1 hour MRI on a 3T Philips Ingenia scanner. During image acquisition, subjects were instructed to keep their eyes closed and move as little as possible. Scans included a 3D MP-RAGE (FOV 250 × 250 × 181 mm, Acq Matrix: 228 × 227 mm, Recon Matrix:240 mm, TE = 3400, TR = 7400), and a 3D fluid-attenuated inversion recovery (FLAIR) image (FOV 270 × 270 × 168 mm, Acq Voxel: 1.13 × 1.13 × 1.12 mm, Recon Voxel: 0.56 × 0.56 × 0.56 mm, TE = 328, TR = 4800, TI = 1650). Diffusion, pCASL and T2* GRE images were also collected but were not included in this analysis.

3.1.5 | Image processing

For volume measurement, T1-weighted images were subjected to automated cortical reconstruction implemented in version 6.0 of the FreeSurfer image analysis suite (surfer.nmr.mgh.harvard.edu). Images were then processed for motion correction, intensity normalization and acquisition artifacts. Images were transformed and stripped of non-brain tissue for normalization into Talariach space for morphometric estimations. Images underwent cortical surface parcellation and subcortical volume-based segmentation. Estimates of cortical and hippocampal volume were obtained using this automated algorithm of subcortical segmentation. Data were visually inspected at key steps for errors preceding the analyses.

FLAIR lesion volume was calculated using the lesion growth algorithm[59] as implemented in the LST open source toolbox version 3.0.0 for SPM. Our computations were completed with MATLAB R2019a and SPM12. T1 images were co-registered to the FLAIR image and lesion maps were calculated based on a user-determined threshold (kappa, 0.3). Lesion volume outcome is reported as a percentage of lesion volume over total brain volume.

3.1.6 | Statistical analysis

All variables were evaluated across disease groups using multivariate analysis of variance (MANOVA). Pearson correlation was used to evaluate the relationship between H_2S metabolites and cognitive and imaging outcome measures. These analyses were performed using SPSS version 26.

We used mediation analysis to test the hypothesis that the effect of a predictor variable (% lesion volume) on an outcome (ADAS score) operated fully or in part through an intervening mediator (total sulfide[60]). Mediation analysis was performed using the PROCESS SPSS macro provided by Hayes and Preacher to perform such analysis.[61]

We also performed ROC analysis to illustrate the ability of H_2S metabolites to distinguish ADRD and control groups using GraphPad Prism v8.4.2 (GraphPad Software, San Diego, California USA). An alpha level of 0.05 was used to determine statistical significance. Outliers were defined as any data point that was > 3SD from the group mean.

To generate decision trees,[57] we used the rpart algorithm (https://cran.r-project.org/web/packages/rpart/rpart.pdf), a regression and classification tree induction algorithm that included the following variables: diagnosis; age; years of education; % hippocampal lesion, and ventricle volume; as well as free, acid-labile, bound, and total H_2S. We used 10-fold cross-validation to reduce the chances of model overfit. In addition, we produced a decision tree based on the H_2S variables alone. Because the control group was larger than the ADRD group the decision tree analysis was performed again using the MRI subgroup.

3.2 | Sodium fluorescein (Na-F) extravasation in mice

In vivo endothelial barrier function was evaluated in C57BL/6 J wild-type and CSE knockout mice[47] using Sodium Fluorescein (Na-F; Sigma, Cat. #F-6377) extravasation as described[30] with modifications. All procedures for handling animals complied with the Guide for Care and Use of Laboratory Animals and were approved by the Institutional Animal Care and Use Committee of LSU Health Sciences Center-Shreveport. All animals were cared for according to the National Institutes of Health guidelines for the care and use of laboratory animals. Briefly, mice under isoflurane anesthesia were injected with 5% Na-F in saline via tail vein (0.4 mg/kg) and were humanely euthanized after 20 minutes. Blood was collected from the inferior vena cava, and the vasculature was thoroughly perfused via the heart with phospate buffered saline (PBS). The brain and lungs were dissected and homogenized in PBS (1 ul/mg) using a tissue homogenizer (Thomas scientific, Swedesboro, NJ). Lysates were mixed with equal volumes of 50% trichloroacetic acid (Sigma, Cat# T-6399), and plasma was mixed with 9 volumes of 20% trichloroacetic acid. All samples were held at 4°C overnight to precipitate protein and were then centrifuged at 12,000 g for 20 minutes. Two volumes of 1X Tris-borate-EDTA buffer (Sigma, Cat# T4415) were added to every volume of supernatant, and pH adjusted to 7.5 to 8.5 using NaOH. Two-fold dilutions were prepared for each sample in Tris-borate-EDTA buffer and fluorescence measured at 485/538 nm and compared to known Na-F standards. The amount of Na-F in samples was calculated in samples where fluorescence was in the linear range. Final results were normalized to plasma and presented as fold changes.

3.3 | Detailed results

3.3.1 | Participant characteristics

Participant characteristics are shown in Table 1. One outlier ADRD subject was excluded based on MRI; therefore, final sample sizes were 15 ADRD and 42 controls. We had an MRI subset of 12 ADRD and 19 controls after one ADRD subject was excluded due to contraindications for MRI and two because of an appointment that was canceled due to COVID-19 closures. There were no significant differences between ADRD and control subjects for age ($F(1, 55) = 0.12$, $P = .73$) or years of education ($F(1,55) = 2.54$, $P = .12$). The ADRD group had significantly higher ADAS-cog scores ($F(1,55) = 93.75$, $P < .001$), indicating poorer cognitive performance.

3.3.2 | Group differences in H_2S metabolites imaging and outcomes

The ADRD group had significantly increased levels of H_2S metabolites (Figure 1). Acid-labile ($F(1,55) = 25.99$, $P < .0022$), bound ($F(1,55) = 29.69$, $P < .0001$), and total sulfide ($F(1,55) = 79.12$, $P < .0001$) were all elevated in the dementia group compared to controls. Free sulfide was not significantly different across groups ($F(1,55) = 5.11$, $P = .31$).

We found differences across groups in MRI outcome measures. Total brain volume was significantly reduced in ADRD (939 (105) mm^3) compared to controls (1029 (101) mm^3; $F(1,30) = 5.73$, $P = .023$). We therefore normalized hippocampal, total gray, and white matter, FLAIR lesion and ventricular volumes by dividing these measures by total volume to obtain a percentage. The ADRD group (Mean(SD) = 0.67 (.073)%) had significantly reduced % hippocampal volume compared to controls (0.72 (.053)%; $F(1, 30) = 5.89$, $P = .022$) as well as increased ventricular size (ADRD = 3.61 (1.9)%, Control = 2.12 (1.6)%; $F(1,30) = 7.360$, $P = .011$). There were no significant differences across groups for % gray matter (ADRD = 54.68 (2.96)%, Control = 55.99 (1.48)%; $F(1,30) = 2.65$, $P = .116$) nor % white matter volume (ADRD = 42.49 (2.81)%, Control = 41.26 (1.43)%; $F(1,30) = 2.61$, $P = .114$). Percent FLAIR lesion volume was significantly larger in the ADRD group (0.76 (0.72)%) versus controls (0.17 (0.16)%; $F(1,30) = 11.99$, $P = .002$).

3.3.3 | Correlation and classification

Correlation analysis revealed a significant relationship between H_2S metabolites and cognitive function (Figure 2 and Table 2). ADAS-cog score was significantly positively correlated with acid-labile ($r(56) = 0.596$, $P < .0001$) and bound sulfane sulfur ($r(56) = 0.436$, $P = .001$), as well as total sulfide pools ($r(56) = 0.681$, $P < .0001$) (Figure 2**A** and Table 2) indicating that poorer cognitive performance was associated with higher metabolite levels. FLAIR lesion volume was significantly correlated with ADAS-cog score ($r(30) = 0.687$, $P < .0001$) (Table 2). Lesion volume was also significantly positively correlated with acid-labile ($r(30) = 0.588$, $P < .0001$) and total sulfide ($r(30) = 0.452$, $P < .011$) (Figure 2**B**), indicating that greater lesion volume was associated with higher sulfide metabolite levels. Importantly, neither ADAS-cog nor lesion volume were correlated with free sulfide (Figure 2 and Table 2).

Mediation analysis revealed that total H_2S mediated the effect of lesion volume on cognitive function (Figure 2C). First, linear regression results showed that the relationship between % FLAIR lesion volume and total H_2S was significant (a', b = 0.0036, SE = 0.0013, $P = .0107$). Second, the relationship between total sulfide and ADAS-cog score was significant (b', b = 1523, SE = 406, $P = .0008$). Finally, lesion volume was a significant predictor of ADAS-cog score (c', b = 11.2, SE = 3.2, $P = .002$). Using a bootstrap estimation approach with 5000 samples[62] we determined that the indirect coefficient was significant (b = 638.4, SE = 299.7, 95% CI = 53.9-1268.4). Our findings indicate partial mediation, with a large (49%) proportion of the effect of lesion volume on ADAS-cog score operating indirectly through total sulfide.

ROC curve analysis revealed significant diagnostic performance for acid-labile, bound, and total sulfide (Figure 3). Free sulfide ROC curve analysis results were not statistically significant (area under the curve AUC = 0.58; 95% confidence interval: 0.42 to 0.75) (**panel 3A**). Discriminative capability for acid-labile H_2S was significant with AUC = 0.76, 95% confidence interval: 0.59 to 0.92 (**panel 3B**). However, much higher discriminative ability was noted with bound (AUC = 0.89, 95% confidence interval: 0.80 to 0.97; **panel 3C**) and total sulfide (AUC = 0.94, 95% confidence interval: 0.92 to 1.000; **panel 3D**), respectively.

Classification analysis using all variables (12 variables including demographic, MRI, and H_2S metabolites) provided a decision tree that had a single level consisting of total sulfide (Figure 4**A**). The tree had an accuracy of 93%, a sensitivity of 80%, a specificity of 98%, a positive predictive value of 92% and a negative predictive value of 93% (Figure 4**B**). Removing MRI variables yielded an identical result. Reducing the number of subjects to those who underwent MRI in order to reduce oversampling of control subjects resulted in slightly reduced accuracy of 90.3%, a positive predictive value of 91%, and a negative predictive value of 90% (Figure 4**B**). Again, exclusion of the MRI variables did not change model performance.

3.3.4 | CSE knockout mice exhibit reduced vascular permeability

Using Na-F solute permeation as a measure of vascular barrier function, we found striking improvements in blood-brain barrier of CSE knockout mice compared to wild-type controls (Figure 5). Interestingly, these improvements in barrier were also seen in the lung and therefore appear to reflect a generalized improvement in vascular barrier, which is not limited to the central nervous system, produced by reduction in H_2S and its metabolites. Mice with this phenotype also have significant reductions in circulating sulfide species. When taken together with our previous report[47] that endothelial cells exposed to per- and

polysulfides show significantly diminished solute barrier, these data show that an environmental sulfide burden predicts endothelial barrier dysfunction. Consequently, the finding that our ADRD subjects have significantly higher plasma sulfides is consistent with a hypothesis in which sulfides in the vascular compartment might drive BBB disturbances that contribute to the initiation and progression of ADRD cognitive dysfunction. Our finding that FLAIR signatures in ADRD are consistent with microvascular derangement also fit this "sulfide" model, however future, prospective studies which can validate relationships between the extent of clinical sulfide burden and ADRD disease severity are still required.

ACKNOWLEDGMENTS

This work was supported by an Institutional Development Award from the National Institutes of General Medical Sciences of the National Institutes of Health under grant number 3P2012130701A1S1 and HL149264-01A1.

CONFLICT OF INTEREST

The authors have no conflicts. A provisional patent was filed based on the findings of this study.

REFERENCES

1. Hardy J, Bogdanovic N, Winblad B, et al. Pathways to Alzheimer's disease. *J Intern Med*. 2014;275:296-303.
2. Hardy JA, Higgins GA. Alzheimer's disease: the amyloid cascade hypothesis. *Science*. 1992;256:184-185.
3. Pluta R, Ulamek-Koziol M, Januszewski S, Czuczwar SJ. Tau Protein Dysfunction after Brain Ischemia. *J Alzheimers Dis*. 2018;66:429-437.
4. Attems J, Jellinger KA. The overlap between vascular disease and Alzheimer's disease–lessons from pathology. *BMC Med*. 2014;12:206.
5. Thal DR, Ghebremedhin E, Orantes M, Wiestler OD. Vascular pathology in Alzheimer disease: correlation of cerebral amyloid angiopathy and arteriosclerosis/lipohyalinosis with cognitive decline. *J Neuropathol Exp Neurol*. 2003;62:1287-1301.
6. Hachinski V, Einhaupl K, Ganten D, et al. Preventing dementia by preventing stroke: the Berlin Manifesto. *Alzheimers Dement*. 2019;15:961-984.
7. Iadecola C. Neurovascular regulation in the normal brain and in Alzheimer's disease. *Nat Rev Neurosci*. 2004;5:347-360.
8. Iadecola C. The pathobiology of vascular dementia. *Neuron*. 2013;80:844-866.
9. Zlokovic BV. Neurovascular pathways to neurodegeneration in Alzheimer's disease and other disorders. *Nat Rev Neurosci*. 2011;12:723-738.
10. Kalaria RN, Akinyemi R, Ihara M. Does vascular pathology contribute to Alzheimer's changes? *J Neurol Sci*. 2012;322:141-147.
11. Reitz C, Tang MX, Manly J, Mayeux R, Luchsinger JA. Hypertension and the risk of mild cognitive impairment. *Arch Neurol*. 2007;64:1734-1740.
12. Skoog I, Gustafson D. Update on hypertension and Alzheimer's disease. *Neurol Res*. 2006;28:605-611.
13. Clark LR, Koscik RL, Allison SL, et al. Hypertension and obesity moderate the relationship between beta-amyloid and cognitive decline in midlife. *Alzheimers Dement*. 2019;15:418-428.
14. Jefferson AL, Cambronero FE, Liu D, et al. Higher aortic stiffness is related to lower cerebral blood flow and preserved cerebrovascular reactivity in older adults. *Circulation*. 2018;138:1951-1962.
15. Roher AE, Esh C, Rahman A, Kokjohn TA, Beach TG. Atherosclerosis of cerebral arteries in Alzheimer's disease. *Stroke*. 2004;35:2623-2627.
16. Barnes DE, Yaffe K. The projected effect of risk factor reduction on Alzheimer's disease prevalence. *Lancet Neurol*. 2011;10:819-828.
17. Gronek P, Balko S, Gronek J, et al. Physical activity and Alzheimer's disease: a narrative review. *Aging Dis*. 2019;10:1282-1292.
18. Emrani S, Lamar M, Price CC, et al. Alzheimer's/Vascular spectrum dementia: classification in addition to diagnosis. *J Alzheimers Dis*. 2020;73:63-71.
19. Alzheimer's Association Calcium Hypothesis W. Calcium hypothesis of Alzheimer's disease and brain aging: a framework for integrating new evidence into a comprehensive theory of pathogenesis. *Alzheimers Dement* 2017, 13:178-182 e17.
20. Khachaturian ZS. The role of calcium regulation in brain aging: reexamination of a hypothesis. *Aging (Milano)*. 1989;1:17-34.
21. Khachaturian ZS. Calcium hypothesis of Alzheimer's disease and brain aging. *Ann N Y Acad Sci*. 1994;747:1-11.
22. Jack CR Jr, Knopman DS, Jagust WJ, et al. Hypothetical model of dynamic biomarkers of the Alzheimer's pathological cascade. *Lancet Neurol*. 2010;9:119-128.
23. Veitch DP, Weiner MW, Aisen PS, et al. Alzheimer's disease neuroimaging I: understanding disease progression and improving Alzheimer's disease clinical trials: recent highlights from the Alzheimer's disease neuroimaging initiative. *Alzheimers Dement*. 2019;15:106-152.
24. Pan LL, Qin M, Liu XH, Zhu YZ. The role of hydrogen sulfide on cardiovascular homeostasis: an overview with update on immunomodulation. *Front Pharmacol*. 2017;8:686.
25. Yong QC, Choo CH, Tan BH, Low CM, Bian JS. Effect of hydrogen sulfide on intracellular calcium homeostasis in neuronal cells. *Neurochem Int*. 2010;56:508-515.
26. Kolluru GK, Shen X, Kevil CG. Reactive sulfur species: a new redox player in cardiovascular pathophysiology. *Arterioscler Thromb Vasc Biol*. 2020;40:874-884.
27. Ishigami M, Hiraki K, Umemura K, Ogasawara Y, Ishii K, Kimura H. A source of hydrogen sulfide and a mechanism of its release in the brain. *Antioxid Redox Signal*. 2009;11:205-214.
28. Abe K, Kimura H. The possible role of hydrogen sulfide as an endogenous neuromodulator. *J Neurosci*. 1996;16:1066-1071.
29. Kimura H. Physiological role of hydrogen sulfide and polysulfide in the central nervous system. *Neurochem Int*. 2013;63:492-497.
30. Jiang Z, Li C, Manuel ML, et al. Role of hydrogen sulfide in early blood-brain barrier disruption following transient focal cerebral ischemia. *PLoS One*. 2015;10:e0117982.
31. He JT, Li H, Yang L, Mao CY. Role of hydrogen sulfide in cognitive deficits: evidences and mechanisms. *Eur J Pharmacol*. 2019;849:146-153.
32. Kumar M, Sandhir R. Neuroprotective effect of hydrogen sulfide in hyperhomocysteinemia is mediated through antioxidant action involving Nrf2. *Neuromolecular Med*. 2018;20:475-490.
33. Giuliani D, Ottani A, Zaffe D, et al. Hydrogen sulfide slows down progression of experimental Alzheimer's disease by targeting multiple pathophysiological mechanisms. *Neurobiol Learn Mem*. 2013;104:82-91.
34. Vandini E, Ottani A, Zaffe D, et al. Mechanisms of hydrogen sulfide against the progression of severe Alzheimer's disease in transgenic mice at different ages. *Pharmacology*. 2019;103:50-60.
35. Fan H, Guo Y, Liang X, et al. Hydrogen sulfide protects against amyloid beta-peptide induced neuronal injury via attenuating inflammatory responses in a rat model. *J Biomed Res*. 2013;27:296-304.
36. Wardlaw JM, Smith EE, Biessels GJ, et al, nEuroimaging STfRVco. Neuroimaging standards for research into small vessel disease and its contribution to ageing and neurodegeneration. *Lancet Neurol*. 2013;12:822-838.

37. Moncada S, Higgs EA. Nitric oxide and the vascular endothelium. *Handb Exp Pharmacol*. 2006:213-254.
38. Tripathi MK, Kartawy M, Amal H. The role of nitric oxide in brain disorders: autism spectrum disorder and other psychiatric, neurological, and neurodegenerative disorders. *Redox Biol*. 2020;34:101567.
39. Kamoun P, Belardinelli MC, Chabli A, Lallouchi K, Chadefaux-Vekemans B. Endogenous hydrogen sulfide overproduction in down syndrome. *Am J Med Genet A*. 2003;116A:310-311.
40. Ide M, Ohnishi T, Toyoshima M, et al. Excess hydrogen sulfide and polysulfides production underlies a schizophrenia pathophysiology. *EMBO Mol Med*. 2019;11:e10695.
41. Kolluru GK, Bir SC, Yuan S, et al. Cystathionine gamma-lyase regulates arteriogenesis through NO-dependent monocyte recruitment. *Cardiovasc Res*. 2015;107:590-600.
42. Peng YJ, Nanduri J, Raghuraman G, et al. H2S mediates O2 sensing in the carotid body. *Proc Natl Acad Sci U S A*. 2010;107:10719-10724.
43. Peers C, Smith IF, Boyle JP, Pearson HA. Remodelling of Ca2+ homeostasis in type I cortical astrocytes by hypoxia: evidence for association with Alzheimer's disease. *Biol Chem*. 2004;385:285-289.
44. Santisteban MM, Iadecola C. Hypertension, dietary salt and cognitive impairment. *J Cereb Blood Flow Metab*. 2018;38:2112-2128.
45. Huang B, Chen CT, Chen CS, Wang YM, Hsieh HJ, Wang DL. Laminar shear flow increases hydrogen sulfide and activates a nitric oxide producing signaling cascade in endothelial cells. *Biochem Biophys Res Commun*. 2015;464:1254-1259.
46. Yuan S, Yurdagul A Jr, Peretik JM, et al. Cystathionine gamma-Lyase modulates flow-dependent vascular remodeling. *Arterioscler Thromb Vasc Biol*. 2018;38:2126-2136.
47. Yuan S, Pardue S, Shen X, Alexander JS, Orr AW, Kevil CG. Hydrogen sulfide metabolism regulates endothelial solute barrier function. *Redox Biol*. 2016;9:157-166.
48. Sweeney MD, Montagne A, Sagare AP, et al. Vascular dysfunction-The disregarded partner of Alzheimer's disease. *Alzheimers Dement*. 2019;15:158-167.
49. Frisoni GB, Boccardi M, Barkhof F, et al. Strategic roadmap for an early diagnosis of Alzheimer's disease based on biomarkers. *Lancet Neurol*. 2017;16:661-676.
50. Rajpal S, Katikaneni P, Deshotels M, et al. Total sulfane sulfur bioavailability reflects ethnic and gender disparities in cardiovascular disease. *Redox Biol*. 2018;15:480-489.
51. Liu XQ, Liu XQ, Jiang P, Huang H, Yan Y. Plasma levels of endogenous hydrogen sulfide and homocysteine in patients with Alzheimer's disease and vascular dementia and the significance thereof. *Zhonghua Yi Xue Za Zhi*. 2008;88:2246-2249.
52. Shen X, Pattillo CB, Pardue S, Bir SC, Wang R, Kevil CG. Measurement of plasma hydrogen sulfide in vivo and in vitro. *Free Radic Biol Med*. 2011;50:1021-1031.
53. Shen X, Peter EA, Bir S, Wang R, Kevil CG. Analytical measurement of discrete hydrogen sulfide pools in biological specimens. *Free Radic Biol Med*. 2012;52:2276-2283.
54. Kautzky A, Seiger R, Hahn A, et al. Prediction of autopsy verified neuropathological change of Alzheimer's disease using machine learning and MRI. *Front Aging Neurosci*. 2018;10:406.
55. Struyfs H, Molinuevo JL, Martin JJ, De Deyn PP, Engelborghs S. Validation of the AD-CSF-index in autopsy-confirmed Alzheimer's disease patients and healthy controls. *J Alzheimers Dis*. 2014;41:903-909.
56. Brickman AM, Tosto G, Gutierrez J, et al. An MRI measure of degenerative and cerebrovascular pathology in Alzheimer disease. *Neurology*. 2018;91:e1402-e12.
57. Kelly C, Hahn C. *Clinical Psychology*. Waltham Abbey Essex, UK: ED-Tech Press; 2019. https://books.google.com/books/about/Clinical_Psychology.html?id=VuTEDwAAQBAJ
58. Monllau A, Pena-Casanova J, Blesa R, et al. Diagnostic value and functional correlations of the ADAS-Cog scale in Alzheimer's disease: data on NORMACODEM project. *Neurologia*. 2007;22:493-501.
59. Schmidt P, Gaser C, Arsic M, et al. An automated tool for detection of FLAIR-hyperintense white-matter lesions in Multiple Sclerosis. *Neuroimage*. 2012;59:3774-3783.
60. Kenny DA, Mediation. 2018. http://davidakenny.net/cm/mediate.htm
61. Hayes AF, The PROCESS macro for SPSS, SAS, and R. 2019. http://www.processmacro.org
62. Shrout PE, Bolger N. Mediation in experimental and nonexperimental studies: new procedures and recommendations. *Psychol Methods*. 2002;7:422-445.

How to cite this article: Disbrow E, Stokes KY, Ledbetter C, **et al.** Plasma hydrogen sulfide: A biomarker of Alzheimer's disease and related dementias. *Alzheimer's Dement*. 2021;17:1391–1402. https://doi.org/10.1002/alz.12305